# nature physics

**Article** 

https://doi.org/10.1038/s41567-024-02517-w

# Topological phase transition between Jain states and daughter states of the $\nu=1/2$ fractional quantum Hall state

Received: 21 August 2023

Accepted: 17 April 2024

Published online: 27 May 2024



S. K. Singh C. Wang , C. T. Tai, C. S. Calhoun, K. A. Villegas Rosales, P. T. Madathil, A. Gupta , K. W. Baldwin, L. N. Pfeiffer & M. Shayegan

The even-denominator fractional quantum Hall state at a filling factor of v = 1/2 is an intriguing many-body phase in two-dimensional electron systems, as it appears in the ground state rather than an excited Landau level. It is observed in wide quantum wells where the electrons have a bilayer charge distribution with finite tunnelling between the layers. Whether this state takes an Abelian two-component form or a non-Abelian one-component form has been debated since its experimental discovery. Here we report the observation of the v = 1/2 state that is flanked by numerous Jain-sequence composite fermion states at  $v = p/(2p \pm 1)$  up to v = 8/17 and 9/17. As we raise the density, the v = 1/2 state is strengthened, its energy gap increases up to 4 K and, at the same time, the 8/17 and 7/13 states abruptly become stronger than their neighbouring high-order fractions. The states at v = 8/17 and 7/13 are the theoretically predicted, simplest daughter states of the one-component Pfaffian v = 1/2 state. This means that our data suggest a topological phase transition of 8/17 and 7/13 states from the Jain-sequence states to the daughter states of the Pfaffian.

Even-denominator fractional quantum Hall states (FQHSs) at half-filled Landau levels (LLs) are of paramount interest currently as they are generally believed to possess quasiparticles that obey non-Abelian statistics and be of potential use in fault-tolerant, topological quantum computing<sup>1</sup>. They are predominantly observed in two-dimensional electron systems (2DESs) at a half-filled, excited-state (N = 1) LL, where the node in the in-plane wavefunction softens the Coulomb interaction and allows for a pairing of flux-particle composite fermions<sup>1-13</sup>. This is in contrast to the half-filled N = 0 LL, namely, at an LL filling factor of v = 1/2, where the composite fermions form a compressible Fermi sea, and the FQHSs are observed at odd-denominator fillings  $v = p/(2p \pm 1)$ on the flanks of v = 1/2 (p is an integer)<sup>14</sup>. However, in 1992, not long after the first observation of the even-denominator FQHS in an  $N = 1LL^2$ , an FQHS at v = 1/2 was reported in 2DESs confined to either a single, wide GaAs quantum well (QW)<sup>15</sup> or to a GaAs double-QW structure<sup>16</sup>. The 1/2 FQHS in the double-QW structure, where the tunnelling between the two QWs is negligible, is understood<sup>17</sup> to be the two-component, Halperin–Laughlin  $\Psi_{331}$  state<sup>18</sup>, which is Abelian. The origin of the 1/2 FQHS in the wide QWs, on the other hand, has been a subject of debate. Initially, it was argued to be a one-component Pfaffian state<sup>19,20</sup>, but the follow-up experiments<sup>21,22</sup> and other theories<sup>17,23,24</sup> suggested a two-component state, with the components being the layer or sub-band degrees of freedom. However, most recent experiments and theories favour a one-component Pfaffian state<sup>25–28</sup>. Evidently, the relatively large layer thickness of electrons in a wide QW softens the short-range component of the Coulomb interaction and allows for composite fermion pairing.

The dichotomy of the v = 1/2 FQHS observed in wide GaAs QWs is highlighted in Fig. 1. Figure 1a depicts the experimental geometry, and Fig. 1b shows the charge distribution (red) and potential (black), calculated by self-consistently solving the Poisson and Schrödinger equations. The results are for electrons confined to a 72.5-nm-wide GaAs QW at three electron densities, namely, n = 0.40, 1.40 and

Department of Electrical and Computer Engineering, Princeton University, Princeton, NJ, USA. —e-mail: sksingh@princeton.edu; shayegan@princeton.edu

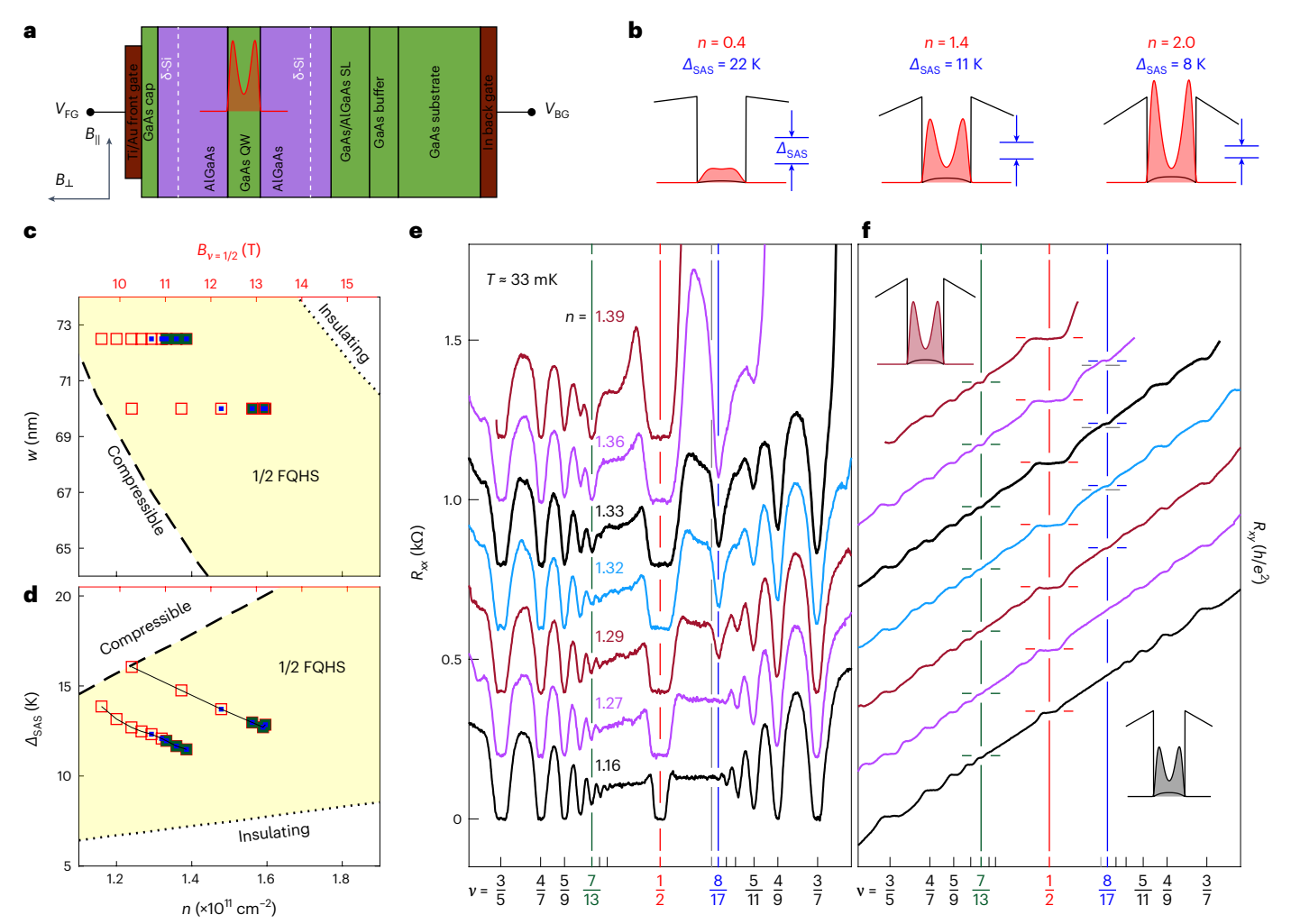


**Fig. 1** | **Evolution of two-dimensional electrons in a wide QW with varying densities. a**, Sketch of a typical, modulation-doped GaAs QW with back and front gates that are used to tune the electron density and maintain the charge distribution symmetric. **b**, Self-consistent charge distribution (red) and potential (black) for a 2DES confined to a 72.5-nm-wide GaAs QW for different n values, as indicated. As n is increased, the 2DES becomes more 'bilayer like', with reduced interlayer tunnelling ( $\Delta_{SAS}$ ). **c.d**, Phase diagrams showing the region (marked in yellow) in which the 1/2 FQHS is stabilized for different QW widths (w) and  $\Delta_{SAS}$  as a function of n. The parameters for which we observe 1/2 FQHSs in our samples agree well with these phase diagrams. The red open squares mark the points where we observe a 1/2 FQHS, whereas the blue and green squares indicate where

we observe the anomalously strong FQHSs at v=8/17 and 7/13, respectively. **e**, **f**, Longitudinal  $(R_{xx})$  (**e**) and Hall  $(R_{xy})$  (**f**) resistances versus inverse filling factor of our sample at  $T\approx 33$  mK for  $1.16 \le n \le 1.39$ , showing the evolution of FQHSs in N=0 LL. Traces are vertically offset for clarity. We normalize the x axes by the density and show the data as a function of the inverse filling factor  $1/v=eB_\perp/nh$ , where  $B_\perp$  is the perpendicular magnetic field (the tick marks show the values of v). We observe anomalously strong FQHS at v=8/17 and 7/13 as n is increased to 1.29 and 1.33, respectively. The green, red, blue and grey guide lines mark the expected position of  $R_{xx}$  minimum and  $R_{xy}$  plateau for v=7/13, 1/2, 8/17 and 9/19, respectively. The charge distribution for n=1.16 and 1.39 are shown as the bottom and top insets in **f**.

2.00 (units,  $\times 10^{11}$  cm<sup>-2</sup>), which we use throughout this Article. At the smallest densities, the electrons occupy the lowest, symmetric electric sub-band, and have a single-layer-like—although thick—charge distribution. As n is increased, the interelectron repulsion along the growth direction leads to a bilayer-like charge distribution<sup>15,21,22,29-32</sup>. The electron repulsion raises the potential in the QW centre and lowers the energy separation  $\Delta_{\text{SAS}}$  between the symmetric and antisymmetric sub-bands, causing the electrons to occupy both sub-bands. Note that  $\Delta_{\text{SAS}}$  represents tunnelling between the two electron layers. As shown in Fig. 1b, with increasing density, the charge distribution becomes increasingly bilayer like and  $\Delta_{\text{SAS}}$  decreases.

Now, as demonstrated in refs. 21,22,30,31, the ground state at v = 1/2 exhibits a remarkable evolution as the density is raised, from a compressible state to an FQHS and then to an insulating phase (this evolution is depicted in Extended Data Figs. 1a and 2). The intermediate-density range where the 1/2 FQHS is stable critically depends on the QW width (w), leading to a w versus density phase

diagram<sup>21,22</sup>. In Fig. 1c, we present an expanded section of this phase diagram, showing the FQHS region (yellow) separated from the compressible and insulating regions (white) by dashed and dotted curves, respectively (the full phase diagram from ref. 22 is also reproduced in Extended Data Fig. 1b). One can also highlight the stability of 1/2 FQHS in a  $\Delta_{\rm SAS}$  versus density phase diagram (Fig. 1d) (for the full phase diagrams, see figures 5 and 6 in ref. 22; a comprehensive discussion of these phase diagrams is provided in Supplementary Section 1).

How can these diagrams be explained? Equivalently, what is the origin of the 1/2 FQHS observed in wide QWs? For a given w, at very low densities, the charge distribution is single-layer like and a compressible ground state is theoretically expected and observed at v=1/2. At very large densities,  $\Delta_{SAS}$  becomes very small and the electron system essentially breaks into two layers, each with a layer filling factor 1/4. If there is no interlayer interaction, again there should be no FQHS at (total filling factor) v=1/2. If the layers are interacting and  $\Delta_{SAS}$  is sufficiently small, however, the two-component  $\Psi_{331}$  FQHS can become

the ground state<sup>17,23,24</sup>. But what about the intermediate values of  $\Delta_{SAS}$ ? The experimental data show a very robust 1/2 FQHS even when  $\Delta_{SAS}$  is about 50 K (in a GaAs QW with w=41 nm (ref. 22)). It turns out that for sufficiently large  $\Delta_{SAS}$ , there is a fierce competitor<sup>33</sup>, namely, the one-component Pfaffian FQHS<sup>19</sup>. Is the 1/2 FQHS then a one-component or a two-component state? This question has been debated for over 30 years (at very high densities and small  $\Delta_{SAS}$ , there is also the possibility of a bilayer Wigner crystal state; the insulating phases observed in experiments favour this possibility<sup>30–32</sup>).

The experimental data we present here shed new light on the origin of the 1/2 FQHS through the observation of its hierarchical daughter states. The traces in Fig. 1e, f show the longitudinal and Hall  $(R_{yy})$  and  $R_{yy}$ respectively) magnetoresistance traces for the electrons confined to a 72.5-nm-wide GaAs OW at varying densities ranging from n = 1.16 to 1.39. The bottom traces, taken at n = 1.16, exhibit a strong FQHS, with a deep  $R_{xx}$  minimum, and a well-defined and wide  $R_{xy}$  plateau, quantized at  $2h/e^2$ . The observation of a strong 1/2 FQHS in this trace is not surprising as the parameters of the sample (n and w) fall in the regime where an FQHS is indeed expected (Fig. 1c shows the phase diagram). The traces also show numerous odd-denominator FQHSs at  $v = p/(2p \pm 1)$ , namely, at v = 1/3, 2/5, 3/7, 4/9... on the high-field side of v = 1/2, and at v = 2/3, 3/5, 4/7, 5/9... on the low-field side (Extended Data Fig. 4 shows a trace over a bigger field range, showing FQHSs at v = 1/3, 2/5, 2/3, and at other odd-denominator v). These are the Jain-sequence FQHSs, typically seen in very high quality 2DESs with single-layer charge distributions, and can be explained as the integer QHSs of two-flux composite fermions<sup>14</sup>. In single-layer 2DESs, the FQHSs become progressively weaker as v = 1/2 is approached, and terminate in a compressible, composite fermion Fermi sea at v = 1/2. The FQHS sequence observed in the n = 1.16 trace (Fig. 1e) is very similar to what is observed in single-layer systems, with the notable exception that the ground state at v = 1/2 is an incompressible FQHS rather than a compressible Fermi sea. Such high-order FQHSs flanking a 1/2 FQHS have been previously observed in wide GaAs QWs but only at much higher densities<sup>22</sup>. The fact that in Fig. 1e, we see  $R_{xx}$  minima at fractions up to v = 8/17 and 9/17 (p = 8 and 9, respectively) at a relatively low density of n = 1.16 attests to the exceptionally high quality of the present sample<sup>34</sup> (Extended Data Fig. 4 and Methods provide more details).

The behaviour of the FQHSs around the v = 1/2 state changes as we increase the density in our sample. As shown in Fig. 1e, the trace at n = 1.27 looks very similar to the n = 1.16 trace, except that the 1/2FQHS is stronger. But at a slightly higher density, that is, n = 1.29, the  $R_{yy}$  minimum at v = 8/17 suddenly becomes much deeper. In fact, it becomes deeper than the nearby lower-order minima at v = 5/11 and 6/13, and engulfs the neighbouring 7/15 minimum. This behaviour is in sharp contrast to the high-order FQHSs seen in the lower-density traces (Fig. 1e), where the 5/11, 6/13 and  $7/15R_{xx}$  minima are deeper than that at 8/17, as expected for the standard Jain-sequence FQHSs<sup>14</sup>. As we further increase n, the 8/17  $R_{xx}$  minimum becomes even deeper. At n = 1.32 and 1.33, for example, the  $R_{xx}$  minimum at 8/17 is comparable in depth to the minima at v = 4/9 and 3/7. The deep  $8/17 R_{xx}$  minimum for  $1.32 \le n \le 1.36$  is accompanied by a well-developed  $R_{xy}$  plateau, quantized at  $(17/8)(h/e^2)$  (Fig. 1f). It is clear that we are observing a robust FQHS at v = 8/17, which is anomalously strong considering its neighbouring odd-denominator states. At the highest densities (Fig. 1e), the  $R_{xx}$  traces show very large values at small fillings. The 2DES starts to exhibit an insulating phase, which has been documented before and interpreted as a pinned bilayer Wigner crystal<sup>30-32</sup>.

The evolution of FQHSs (Fig. 1e,f) on the high-filling side of v = 1/2 is equally impressive as we increase n. In this case, it is the v = 7/13 FQHS that becomes anomalously strong with increasing n and eventually becomes dominant over its neighbouring FQHSs. It starts to strengthen as n exceeds 1.32 and at n = 1.36 and 1.39, it exhibits a very deep  $R_{xx}$  minimum and an  $R_{xy}$  that is quantized at  $(13/7)(h/e^2)$ .

The anomalous strengthening of the 8/17 and 7/13 FQHSs is particularly remarkable because these are exactly the simplest hierarchical

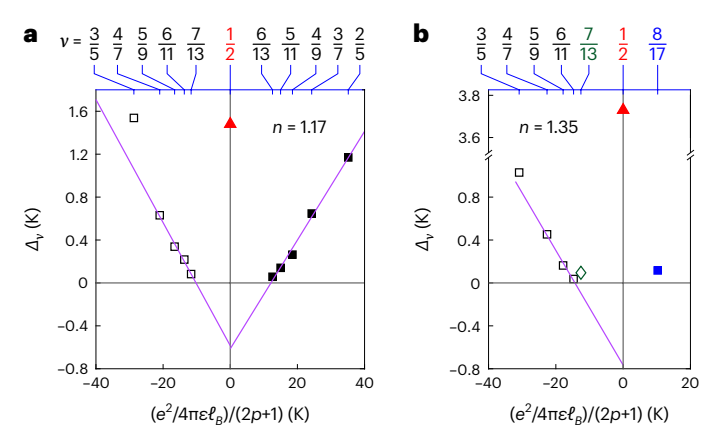
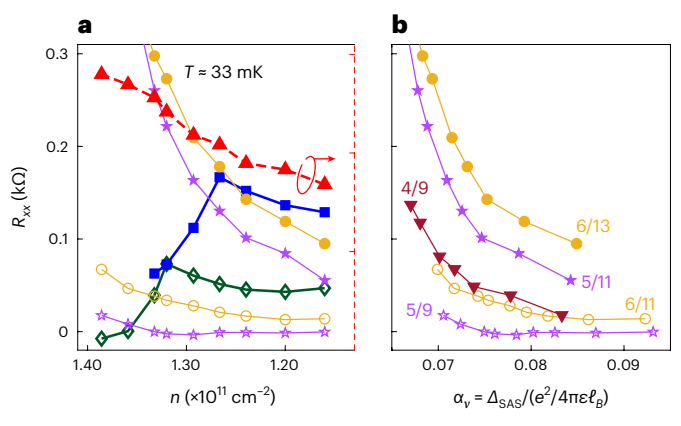


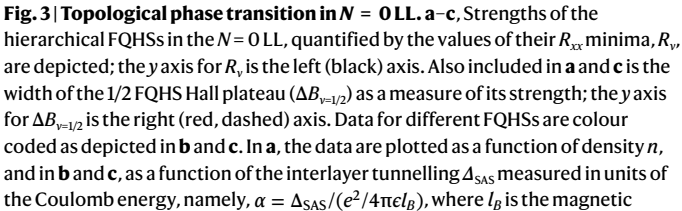
**Fig. 2** | **Energy gaps**  $\Delta_v$  **of FQHSs in** N = 0 **LL.** Measured  $\Delta_v$  are shown as a function of  $(e^2/4\pi\epsilon l_B)/(2p+1)$ , where  $e^2/4\pi\epsilon l_B$  is the Coulomb energy,  $\epsilon$  is the dielectric constant of GaAs,  $l_B$  is the magnetic length at the corresponding fillings and p = v/(1-2v). **a**, n = 1.17. **b**, n = 1.35. As n is raised from 1.17 to 1.35, Jain-sequence FQHSs get weaker owing to the thicker 2DES except for those at v = 7/13 and 8/17, which become anomalously strong. Concomitantly, the v = 1/2 gap increases from 1.48 to 3.73 K

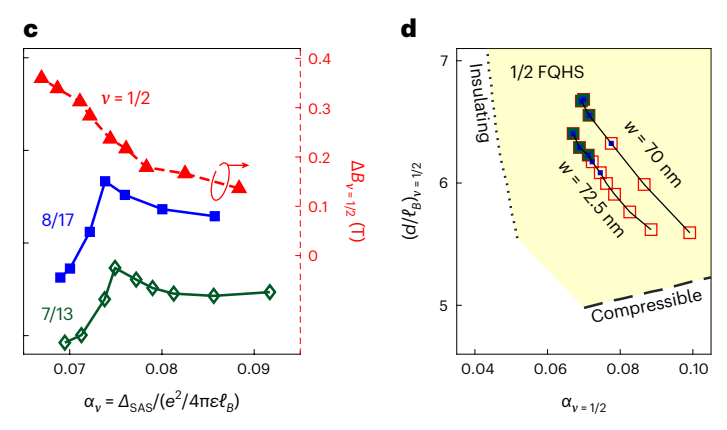
daughter states of the v = 1/2 Pfaffian state predicted by theory<sup>35</sup>. Levin and Halperin constructed a series of hierarchical daughter states for e/4 excitations of the Pfaffian state and showed that the simplest of these states occur at v = 7/13 and 8/17 (ref. 35). In contrast, the hierarchical daughter states of the  $\Psi_{331}$  state occur at  $\nu = 7/13$  and 9/19 (ref. 36), and the daughter states of the anti-Pfaffian occur at v = 6/13 and 9/17(ref. 35) (for a more complete discussion on the daughter states, Supplementary Section 2 discusses the daughter states of  $\Psi_{331}$  and K = 8strong-pairing states have been derived using Wen's K-matrix formulation<sup>36</sup>; the daughter states of the non-Abelian Pfaffian and anti-Pfaffian states have been derived in ref. 35 and are also summarized in Supplementary Table 1). Our observation of the anomalously strong v = 7/13and 8/17 FQHSs flanking a very robust FQHS at v = 1/2 is consistent with a Pfaffian origin for the 1/2 FQHS (note that according to theory<sup>35</sup>, the 8/17 and 7/13 FQHSs are Abelian, even though their parent 1/2 FQHS is non-Abelian).

It is worth noting that in bilayer graphene where even-denominator FQHSs are observed in the N=1LLs, capacitance and magnetotransport studies have recently reported anomalous FQHSs at partial filling factors  $\tilde{v}=7/13$  and 8/17 (refs. 7,8,12) on the flanks of even-denominator FQHSs at v=3/2, 7/2, -5/2 and -1/2, and at  $\tilde{v}=6/13$  and 9/17 at around v=5/2 (ref. 12). These anomalous FQHSs have been interpreted as the hierarchical daughter states of the even-denominator Pfaffian and anti-Pfaffian FQHSs, respectively. In GaAs 2DESs, an anomalous FQHS at  $\tilde{v}=6/13$  at around v=5/2 FQHS was also observed at a very low electron temperature  $^{37}$ ; however, no anomalous FQHS was observed at  $\tilde{v}=9/17$ . A crucial distinction is that in our wide GaAs QW samples, we observe the 1/2 FQHS and its hierarchical daughter FQHSs at 7/13 and 8/17 in the ground (N=0) LL rather than in the excited (N=1) LL. Moreover, in bilayer graphene, no transition is reported at these fillings.

Next, we more closely focus on the evolution of FQHSs (Fig. 1e,f). We begin again with the lowest-density (n=1.16) trace. The Jain-sequence FQHSs observed at  $v=p/(2p\pm1)$  in this trace have the same pattern as in the standard, single-layer 2DESs, namely, they monotonically become weaker as p increases. This trend can be quantitatively observed in Fig. 2a, where we plot the energy gaps  $\Delta_v$ , determined from the temperature dependence of the resistance minimum  $R_{xx} \propto e^{-\Delta_v/2kT}$  (Extended Data Fig. 5). For an ideal 2DES (with zero layer thickness, no LL mixing and no disorder), these gaps are expected to scale as  $\Delta_v = (C/|2p+1|)E_C$  (refs. 14,38), where  $E_C = e^2/4\pi\varepsilon l_B$  is the Coulomb energy,  $I_B = \sqrt{\hbar/eB}$  is the magnetic length at the corresponding fillings,







length at the corresponding fillings. We observe the evidence of phase transitions from the Jain states to the 1/2 FQHS hierarchical daughter states at  $\nu=8/17$  and 7/13 at  $\alpha=0.075$ . **d**, A  $d/l_{\rm B}$  versus  $\alpha$  phase diagram showing where we observe the 1/2 FQHS and the anomalously strong  $\nu=8/17$  and 7/13 FQHSs. Here d is the interlayer distance deduced from the self-consistent calculations at zero magnetic field, and  $l_{\rm B}$  is the magnetic length at  $\nu=1/2$ . The symbols are the same as that in the phase diagrams shown in Fig. 1c,d.

 $C \approx 0.3$  and v = p/(2p + 1). As shown in Fig. 2a, the gaps monotonically get smaller for higher p until they become immeasurably small. This trend is similar to what is experimentally observed and theoretically expected in narrower GaAs QWs where the odd-denominator FQHSs are described as the Jain-sequence FQHSs  $^{39-42}$ . Note that the measured gaps near v = 1/2 extrapolate to a negative value at v = 1/2. This is consistent with previous measurements where the negative intercept is interpreted to reflect broadening due to the sample disorder  $^{39-41}$ . Also consistent with previous studies are the smaller values of the measured gaps in Fig. 2a compared with narrower QWs; the larger effective thickness of the electron layer in the present sample softens the short-range electron–electron interaction and leads to smaller FQHS gaps  $^{41,42}$ . What is, of course, unusual in Fig. 2a and the  $R_{xx}$  trace in Fig. 1e is that there is an FQHS at v = 1/2, even though the high-order FQHSs on its flanks behave the same way as in a standard, although thick, 2DES.

As the density is raised, the traces in Fig. 1e initially reveal a gradual weakening of all the  $v = p/(2p \pm 1)$  FQHSs. This is best seen in Fig. 3a, which shows that values of  $R_{xx}$  minima gradually increase as n is raised, and can be explained to result from the increase in the electron system's effective thickness<sup>41</sup>. As the density is further raised, the  $v = p/(2p \pm 1)$ FQHSs continue to become weaker as evinced from the increase in their  $R_{xx}$  minima values (Fig. 3a), except, of course, the FQHSs at v = 8/17 and 7/13, which suddenly start to strengthen at n = 1.29 and 1.33, respectively (the 8/17 FQHS weakens and disappears at the highest n as an insulating phase engulfs it). If we convert the x axis in Fig. 3a to  $\alpha = \Delta_{SAS}/(e^2/4\pi\epsilon l_B)$ , that is, a dimensionless parameter quantifying the ratio of the tunnelling energy to the in-plane interaction energy, as is commonly done in numerous studies<sup>21,23,24,27,30,31,33</sup>, we find that the sudden strengthening of the 8/17 and 7/13 FQHSs indeed occurs essentially at the same value of  $\alpha \approx 0.075$  (Fig. 3b,c) (in Fig. 3c, although we cannot rule out that some rounding may occur at the transition seen for the 8/17 and 7/13 FQHSs at  $\alpha \approx 0.075$  if more closely spaced data points were available, the transition appears to be fairly abrupt; see, for example, the marked strengthening of the 8/17  $R_{xx}$  minimum in Fig. 1e as the density is raised by approximately 1.5% from 1.27 to 1.29).

The data shown in Fig. 3b,c reveal a clear, sudden transition at 8/17 and 7/13 from Jain-sequence FQHSs to FQHSs that are predicted to be the daughter states of the Pfaffian state<sup>35</sup>. The theory of Levin and Halperin<sup>35</sup> also posits that the two sets are topologically distinct. Our data, therefore, suggest that we are seeing a topological phase transition at  $\nu = 7/13$  and 8/17 from Jain-sequence FQHSs to the

hierarchical daughter FQHSs of the Pfaffian 1/2 FQHS in our sample. This is further reinforced by the measured energy gaps at n=1.35 (Fig. 2b), where the 7/13 FQHS energy gap no longer follows the trend observed for Jain states. Similarly, although the energy gap of 8/17 FQHS was immeasurably small at n=1.17, now it shows an anomalously strong value, contrary to what is expected of Jain states. The Arrhenius plots to extract the energy gaps of FQHSs are presented in Extended Data Figs. 5 and 6.

It is remarkable that in the whole density range of our experiments on this sample, even as the 8/17 and 7/13 FQHSs are undergoing a phase transition, the 1/2 FQHS monotonically becomes stronger as n increases. This is evidenced by the steady increase in the  $R_{xy}$  plateau width  $(\Delta B_v)$  with density (Fig. 3a,c). It is possible that the stability of the 8/17 and 7/13 FQHSs as the daughter states of the 1/2 FQHS requires a minimal strength of the latter. As Fig. 2b illustrates, the 1/2 FQHS at n=1.35 is indeed extremely robust. It has a large energy gap,  $\Delta_{y=1/2}\approx 3.73$  K; this is much larger than the transport gaps reported for any even-denominator FQHS in any semiconducting material platform<sup>6,10,34</sup>, and comparable with the largest gaps reported in bilayer graphene<sup>7,8,12</sup>. This is particularly remarkable, considering that the size of our sample (-16 mm²) is about  $10^6-10^7$  times larger than the typical bilayer graphene samples; the much larger size is important for potential use of these materials as platforms for topological quantum computing.

Next, we present the evolution of FQHSs in our sample by tilting it in the magnetic field and introducing a parallel field component  $(B_{\parallel})$  (Fig. 4b, inset). Owing to its coupling to the out-of-plane orbital motion of electrons,  $B_{\parallel}$  reduces the interlayer tunnelling, qualitatively similar to increasing n (refs. 43,44). Figure 4 reveals that when we tilt the sample at a low density where the strengths of FQHSs follow the Jain-sequence protocol at  $\theta=0$ , anomalously strong FQHSs appear at 8/17 and 7/13 at higher  $\theta$ . The fact that the 8/17 FQHS shows up at a lower  $\theta$  compared with the 7/13 FQHS is qualitatively consistent with the density-dependence data shown in Fig. 1e,f; at a given  $\theta$ , the tunnelling is more suppressed at the field position of the 8/17 FQHS compared with 7/13 because of the larger  $B_{\parallel}$ . It is worth mentioning that although not highlighted, the tilt data in ref. 44 also exhibit clear hints of anomalously strong 8/17 and 7/13 FQHSs (traces at  $\theta=35^{\circ}$  and 37° in Fig. 1 and 10° and 20° in figure 2a of ref. 44).

The abruptness of the transitions at the  $\nu=8/17$  and 7/13 FQHSs (Fig. 3c) suggests that they are of the first order. We also made measurements on a narrower (70-nm-wide) GaAs QW (Extended Data Figs. 2 and 3).

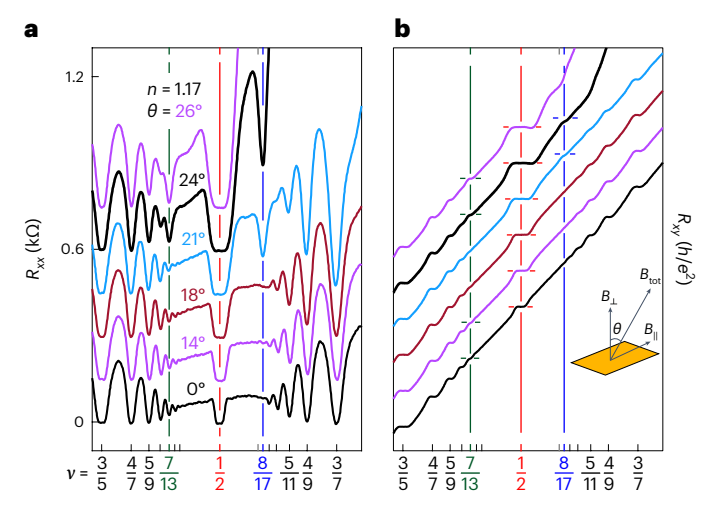


**Fig. 4** | **Effect of in-plane magnetic field. a,b**,  $R_{xx}$  (**a**) and  $R_{xy}$  (**b**) show qualitatively similar behaviour to an increase in the 2DES density. The traces have been vertically offset for clarity. The inset in **b** shows the angle  $\theta$ .

The results confirm our findings for the wider QW and show similar phase transitions, although at slightly larger densities, as summarized in the phase diagrams shown in Figs. 1c,d and 3d. It is indisputable that the exceptional quality and purity of the samples is crucial for our observations (Methods). However, the precise parameters (QW width, density,  $\Delta_{SAS}$  and so on) contained in these phase diagrams are also of paramount importance as they provide experimental input for future studies—both experimental and theoretical—to unravel the microscopic nature of the Pfaffian daughter states, and their relevant transitions at  $\nu = 8/17$  and 7/13.

Finally, two very recent studies have reported capacitance, transport and tunnelling data near the even-denominator FQHSs in bilayer graphene 45,46. They report large energy gaps for the even-denominator FQHSs, and confirm the observation of hierarchical daughter states at partial LL filling factors  $\tilde{v} = 8/17$  and 7/13 in the N = 1 LL in bilayer graphene  $^{7,8,12}$ . Also, in figure 5 of ref. 46, data are shown near the half-filled N = 2 LL. These data have a striking resemblance to the data seen in the N = 0 LL in wide GaAs QW samples at low densities before 8/17 and 7/13 become anomalously strong, namely, they exhibit a relatively robust even-denominator FOHS flanked by numerous odd-denominator FQHSs at  $\tilde{v} = p/(2p \pm 1)$  whose strengths follow the Jain-sequence protocol (see, for example, the traces at n = 1.16 in Fig. 1e, fand Extended Data Figs. 2a and 4). This behaviour for the N = 0 LL in wide GaAs QWs has, of course, been well established and documented in numerous previous reports<sup>21,22</sup>. What is unexpected is that it is now seen in the N = 2 LL of bilayer graphene.

# Online content

Any methods, additional references, Nature Portfolio reporting summaries, source data, extended data, supplementary information, acknowledgements, peer review information; details of author contributions and competing interests; and statements of data and code availability are available at https://doi.org/10.1038/s41567-024-02517-w.

# References

- Nayak, C., Simon, S. H., Stern, A., Freedman, M. & Sarma, S. D. Non-Abelian anyons and topological quantum computation. *Rev. Mod. Phys.* 80, 1083–1159 (2008).
- Willett, R. et al. Observation of an even-denominator quantum number in the fractional quantum Hall effect. *Phys. Rev. Lett.* 59, 1776–1779 (1987).
- Moore, G. & Read, N. Nonabelions in the fractional quantum Hall effect. Nucl. Phys. B 360, 362–396 (1991).

- Read, N. & Green, D. Paired states of fermions in two dimensions with breaking of parity and time-reversal symmetries and the fractional quantum Hall effect. *Phys. Rev. B* 61, 10267–10297 (2000).
- 5. Ki, D. K., Fal'ko, V. I., Abanin, D. A. & Morpurgo, A. F. Observation of even denominator fractional quantum Hall effect in suspended bilayer graphene. *Nano Lett.* **14**, 2135–2139 (2014).
- Falson, J. et al. Even-denominator fractional quantum Hall physics in ZnO. Nat. Phys. 11, 347–351 (2015).
- 7. Li, J. I. A. et al. Even-denominator fractional quantum Hall states in bilayer graphene. *Science* **358**, 648–652 (2017).
- Zibrov, A. A. et al. Tunable interacting composite fermion phases in a half-filled bilayer-graphene Landau level. *Nature* 549, 360–364 (2017).
- Hossain, M. S. et al. Unconventional anisotropic even-denominator fractional quantum Hall state in a system with mass anisotropy. *Phys. Rev. Lett.* 121, 256601 (2018).
- 10. Shi, Q. et al. Odd- and even-denominator fractional quantum Hall states in monolayer WSe<sub>2</sub>. *Nat. Nanotechnol.* **15**, 569–573 (2020).
- 11. Dutta, B. et al. Distinguishing between non-Abelian topological orders in a quantum Hall system. *Science* **375**, 193–197 (2022).
- 12. Huang, K. et al. Valley isospin controlled fractional quantum Hall states in bilayer graphene. *Phys. Rev. X* **12**, 031019 (2022); erratum **12**, 049901 (2022).
- 13. Willett, R. L. et al. Interference measurements of non-Abelian e/4 & Abelian e/2 quasiparticle braiding. *Phys. Rev. X* **13**, 011028 (2023)
- 14. Jain, J. K. Composite Fermions (Cambridge Univ. Press, 2007).
- Suen, Y. W., Engel, L. W., Santos, M. B., Shayegan, M. & Tsui, D. C. Observation of a v=1/2 fractional quantum Hall state in a double-layer electron system. *Phys. Rev. Lett.* 68, 1379–1382 (1992).
- Eisenstein, J. P., Boebinger, G. S., Pfeiffer, L. N., West, K. W. & He, S. New fractional quantum Hall state in double-layer two-dimensional electron systems. *Phys. Rev. Lett.* 68, 1383–1386 (1992).
- 17. He, S., Das Sarma, S. & Xie, X. C. Quantized Hall effect and quantum phase transitions in coupled two-layer electron systems. *Phys. Rev. B* **47**, 4394–4412 (1993).
- 18. Halperin, B. I. Theory of the quantized Hall conductance. *Helv. Phys. Acta* **56**, 75–102 (1983).
- Greiter, M., Wen, X. G. & Wilczek, F. Paired Hall states in double-layer electron systems. *Phys. Rev. B* 46, 9586–9589 (1992).
- Greiter, M., Wen, X. G. & Wilczek, F. Paired Hall states. *Nucl. Phys. B* 374, 567–614 (1992).
- 21. Suen, Y. W., Manoharan, H. C., Ying, X., Santos, M. B. & Shayegan, M. Origin of the *v*=1/2 fractional quantum Hall state in wide single quantum wells. *Phys. Rev. Lett.* **72**, 3405–3408 (1994).
- 22. Shabani, J. et al. Phase diagrams for the stability of the v=1/2 fractional quantum Hall effect in electron systems confined to symmetric, wide GaAs quantum wells. *Phys. Rev. B* **88**, 245413 (2013).
- 23. Peterson, M. R. & Sarma, S. D. Quantum Hall phase diagram of half-filled bilayers in the lowest and the second orbital Landau levels: Abelian versus non-Abelian incompressible fractional quantum Hall states. *Phys. Rev. B* **81**, 165304 (2010).
- Thiebaut, N., Regnault, N. & Goerbig, M. O. Fractional quantum Hall states versus Wigner crystals in wide quantum wells in the half-filled lowest and second Landau levels. *Phys. Rev. B* 92, 245401 (2015).
- Mueed, M. A. et al. Geometric resonance of composite fermions near the v=1/2 fractional quantum Hall state. Phys. Rev. Lett. 114, 236406 (2015).
- Mueed, M. A. et al. Geometric resonance of composite fermions near bilayer quantum Hall states. *Phys. Rev. Lett.* 117, 246801 (2016).

- Zhu, W., Liu, Z., Haldane, F. D. M. & Sheng, D. N. Fractional quantum Hall bilayers at half filling: tunneling-driven non-Abelian phase. *Phys. Rev. B* 94, 245147 (2016).
- Sharma, A., Balram, A. C. & Jain, J. K. Composite-fermion pairing at half-filled and quarter-filled lowest Landau level. *Phys. Rev. B* 109, 035306 (2024).
- 29. Suen, Y. W. et al. Missing integral quantum Hall effect in a wide single quantum well. *Phys. Rev. B* **44**, 5947–5950 (1991).
- Manoharan, H. C., Suen, Y. W., Santos, M. B. & Shayegan, M. Evidence for a bilayer quantum Wigner solid. *Phys. Rev. Lett.* 77, 1813–1816 (1996).
- 31. Shayegan, M., Manoharan, H. C., Suen, Y. W., Lay, T. S. & Santos, M. B. Correlated bilayer electron states. *Semicond. Sci. Technol.* **11**, 1539–1545 (1996).
- Hatke, A. T. et al. Microwave spectroscopic observation of a Wigner solid within the v=1/2 fractional quantum Hall effect. Phys. Rev. B 95, 045417 (2017).
- 33. Halperin, B. I. Theories for v=1/2 in single- and double-layer systems. Surf. Sci. **305**, 1–7 (1994).
- Chung, Y. J. et al. Ultra-high-quality two-dimensional electron systems. Nat. Mater. 20, 632–637 (2021).
- Levin, M. & Halperin, B. I. Collective states of non-Abelian quasiparticles in a magnetic field. Phys. Rev. B 79, 205301 (2009).
- Wen, X. G. Topological orders and edge excitations in fractional quantum Hall states. Adv. Phys. 44, 405–473 (1995).
- Kumar, A., Csáthy, G. A., Manfra, M. J., Pfeiffer, L. N. & West, K. W. Nonconventional odd-denominator fractional quantum Hall states in the second Landau level. *Phys. Rev. Lett.* **105**, 246808 (2010).
- 38. Halperin, B. I., Lee, P. A. & Read, N. Theory of the half-filled Landau level. *Phys. Rev. B* **47**, 7312–7343 (1993).
- Du, R. R., Stormer, H. L., Tsui, D. C., Pfeiffer, L. N. & West, K. W. Experimental evidence for new particles in the fractional quantum Hall effect. *Phys. Rev. Lett.* 70, 2944–2947 (1993).

- Manoharan, H. C., Shayegan, M. & Klepper, S. J. Signatures of a novel Fermi liquid in a two-dimensional composite particle metal. *Phys. Rev. Lett.* 73, 3270–3273 (1994).
- Villegas Rosales, K. A. et al. Fractional quantum Hall effect energy gaps: role of electron layer thickness. *Phys. Rev. Lett.* 127, 056801 (2021).
- 42. Zhao, T., Kudo, K., Faugno, W. N., Balram, A. C. & Jain, J. K. Revisiting excitation gaps in the fractional quantum Hall effect. *Phys. Rev. B* **105**, 205147 (2022).
- 43. Lay, T. S., Jungwirth, T., Smrčka, L. & Shayegan, M. One-component to two-component transition of the *v*=2/3 fractional quantum Hall effect in a wide quantum well induced by an in-plane magnetic field. *Phys. Rev. B* **56**, R7092–R7095 (1997).
- 44. Hasdemir, S. et al. v=1/2 fractional quantum Hall effect in tilted magnetic fields. *Phys. Rev. B* **91**, 045113 (2015).
- 45. Assouline, A. et al. Energy gap of the even-denominator fractional quantum Hall state in bilayer graphene. *Phys. Rev. Lett.* **132**, 046603 (2024).
- Hu, Y. et al. High-resolution tunneling spectroscopy of fractional quantum Hall states. Preprint at https://arxiv.org/abs/2308.05789 (2023).

**Publisher's note** Springer Nature remains neutral with regard to jurisdictional claims in published maps and institutional affiliations.

Springer Nature or its licensor (e.g. a society or other partner) holds exclusive rights to this article under a publishing agreement with the author(s) or other rightsholder(s); author self-archiving of the accepted manuscript version of this article is solely governed by the terms of such publishing agreement and applicable law.

© The Author(s), under exclusive licence to Springer Nature Limited 2024

#### Methods

Our samples, grown using molecular-beam epitaxy, exhibit record-high mobilities of  $\mu \approx 10 \times 10^6$  cm² V<sup>-1</sup> s<sup>-1</sup> for 2DESs confined to wide GaAs QWs where two sub-bands are occupied. This record mobility was achieved by improvements in the vacuum integrity of molecular-beam epitaxy, extensive Al and Ga source purification and doping the sample with Si in doping-well structures<sup>34</sup>.

As discussed in the main text, as well as in other work 15,21,22,29-31 the 2DES in a wide GaAs QW is a particularly flexible and versatile platform as its important parameters, such as the shape of the charge distribution and interlayer tunnelling, can be tuned over a wide range (Fig. 1b). As demonstrated in this study, changes in charge distribution profoundly affect the correlated states of the wide QW, particularly the v = 1/2 FOHS and its daughter states. It is worth highlighting three main advantages of electrons confined to a wide QW over those in a double-QW structure, for example, electrons confined to two GaAs QWs separated by an Al, Ga<sub>1-x</sub>As barrier. First, the potential controlling the tunnelling and the (bilayer) charge distribution in wide QWs is generated by the electrons themselves and can be tuned over a considerable range by changing the electron density. Second, in a double-QW structure, the interfaces between the GaAs QWs and the  $Al_xGa_{1-x}As$  barriers can lead to interface roughness scattering. Third, when interlayer tunnelling is substantial in a double-QW structure, the electron charge distribution penetrates deep into the  $Al_xGa_{1-x}As$  barrier, causing alloy scattering. Moreover, the purity of the  $Al_xGa_{1-x}As$  barrier is not as high as that of a pure GaAs layer<sup>34</sup>. As a result, the electrons in a wide QW suffer much less from disorder, as indeed confirmed by their exceptionally high mobilities, and the display of delicate many-body states.

Samples are prepared for magnetotransport experiments by cleaving a 4 mm  $\times$  4 mm square piece from a two-inch GaAs wafer that has the molecular-beam-epitaxy-grown structure. Eutectic In:Sn is deposited on the sample with a soldering iron and subsequently annealed at 425 °C for 4 min in a reducing environment of 95%:5%  $N_2$ :H $_2$  for making reliable ohmic contacts at the sample's four corners and side midpoints. The front gate consists of a 10-nm-thick layer of Ti plus a 30-nm-thick layer of Au, which are deposited under a high vacuum using an electron-beam evaporator. Indium is melted on the back surface to serve as the back-gate electrode.

The measurements are performed in the van der Pauw geometry using standard lock-in techniques. All the measurements at the base temperature of  $T \approx 33$  mK were made using a 20 nA excitation current; the energy-gap measurements were made using a 50 nA excitation current.

# Data availability

The data that support the plots within this paper and other findings of this study are available from the corresponding authors upon reasonable request. Source data are provided with this paper.

# **Acknowledgements**

We acknowledge support by the US Department of Energy (DOE) Basic Energy Sciences via grant no. DEFG02-00-ER45841 for measurements. the National Science Foundation (NSF) grant nos. DMR 2104771 and ECCS 1906253 for sample characterization and the Eric and Wendy Schmidt Transformative Technology Fund for sample fabrication. The Princeton University portion of this research is funded in part by the Gordon and Betty Moore Foundation's EPiQS Initiative, grant GBMF9615.01, to L.N.P. Our measurements were partly performed at the National High Magnetic Field Laboratory (NHMFL), which is supported by the NSF Cooperative Agreement no. DMR 1644779, by the State of Florida, and by the DOE. This research is funded in part by QuantEmX grant from the Institute for Complex Adaptive Matter and the Gordon and Betty Moore Foundation through grant GBMF9616 to S.K.S., C.W., A.G., C.T.T. and C.S.C. We thank R. Nowell, G. Jones, A. Bangura and T. Murphy at NHMFL for technical assistance, and B. I. Halperin, J. K. Jain, P. Kumar, M. Levin and X.-G. Wen for illuminating discussions.

# **Author contributions**

S.K.S. and M.S. conceived the work. S.K.S., C.W., C.T.T. and C.S.C. performed the low-temperature transport measurements. S.K.S. and K.W.B. fabricated the sample. L.N.P., K.W.B. and A.G. produced the molecular-beam epitaxy samples and characterized them. S.K.S. and M.S. analysed the data and wrote the manuscript with input from all co-authors.

# **Competing interests**

The authors declare no competing interests.

# **Additional information**

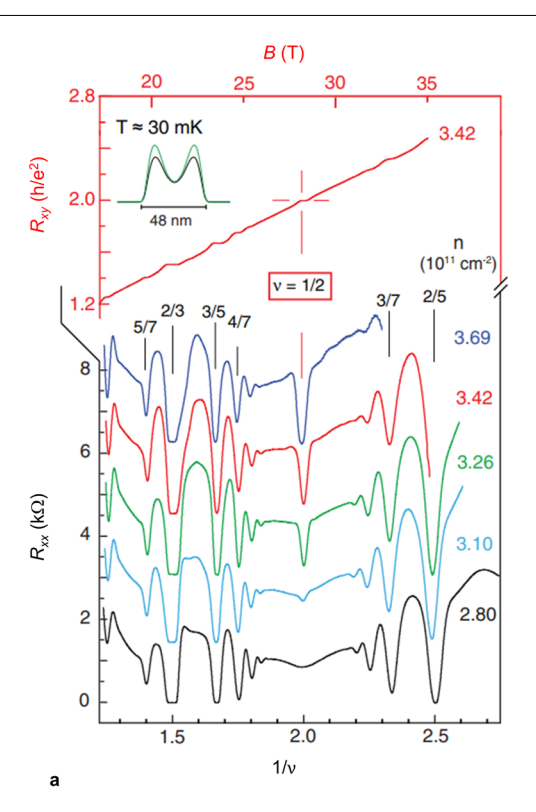
**Extended data** is available for this paper at https://doi.org/10.1038/s41567-024-02517-w.

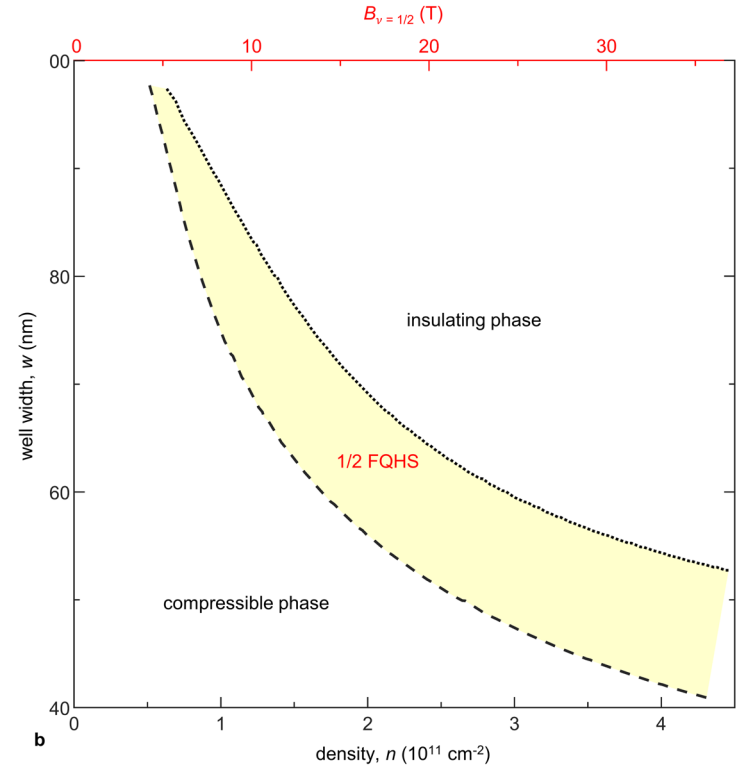
**Supplementary information** The online version contains supplementary material available at https://doi.org/10.1038/s41567-024-02517-w.

**Correspondence and requests for materials** should be addressed to S. K. Singh or M. Shayegan.

**Peer review information** *Nature Physics* thanks Zlatko Papic, and the other, anonymous, reviewer(s) for their contribution to the peer review of this work.

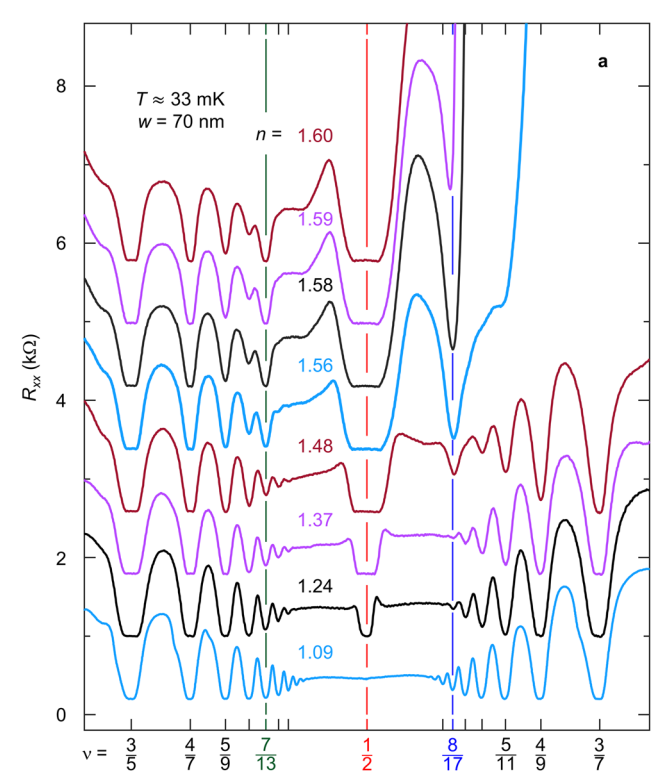
**Reprints and permissions information** is available at www.nature.com/reprints.



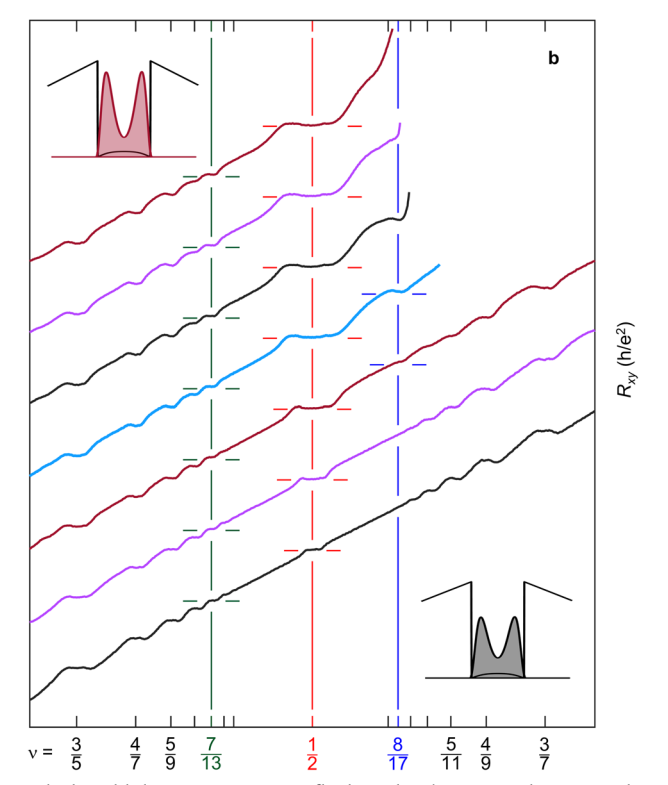


**Extended Data Fig. 1**| **Evolution of the ground state at**  $\nu=1/2$  **in wide GaAs QWs. a**, Longitudinal resistance ( $R_{xx}$ ) of 2D electrons confined to a 48-nm-wide GaAs QW shows the evolution from a compressible composite fermion Fermi sea to an incompressible phase, the 1/2 FQHS, as the 2D electron density is raised symmetrically. Except for the bottom trace, the traces are offset vertically for clarity. The 1/2 FQHS becomes stronger as the density is raised within an intermediate density range as evinced by the  $R_{xx}$  minimum at  $\nu=1/2$  getting deeper and eventually touching zero. The top trace shows the Hall resistance ( $R_{xy}$ ) for  $n=3.42\times10^{11}$  cm $^{-2}$ . Also noteworthy is that the numerous odd-denominator FQHSs at the lowest density n=2.80 are also present together with the strong 1/2 FQHS at higher densities. The relative strengths of the odd-denominator FQHSs suggest that these are the usual Jain-sequence states at all densities.

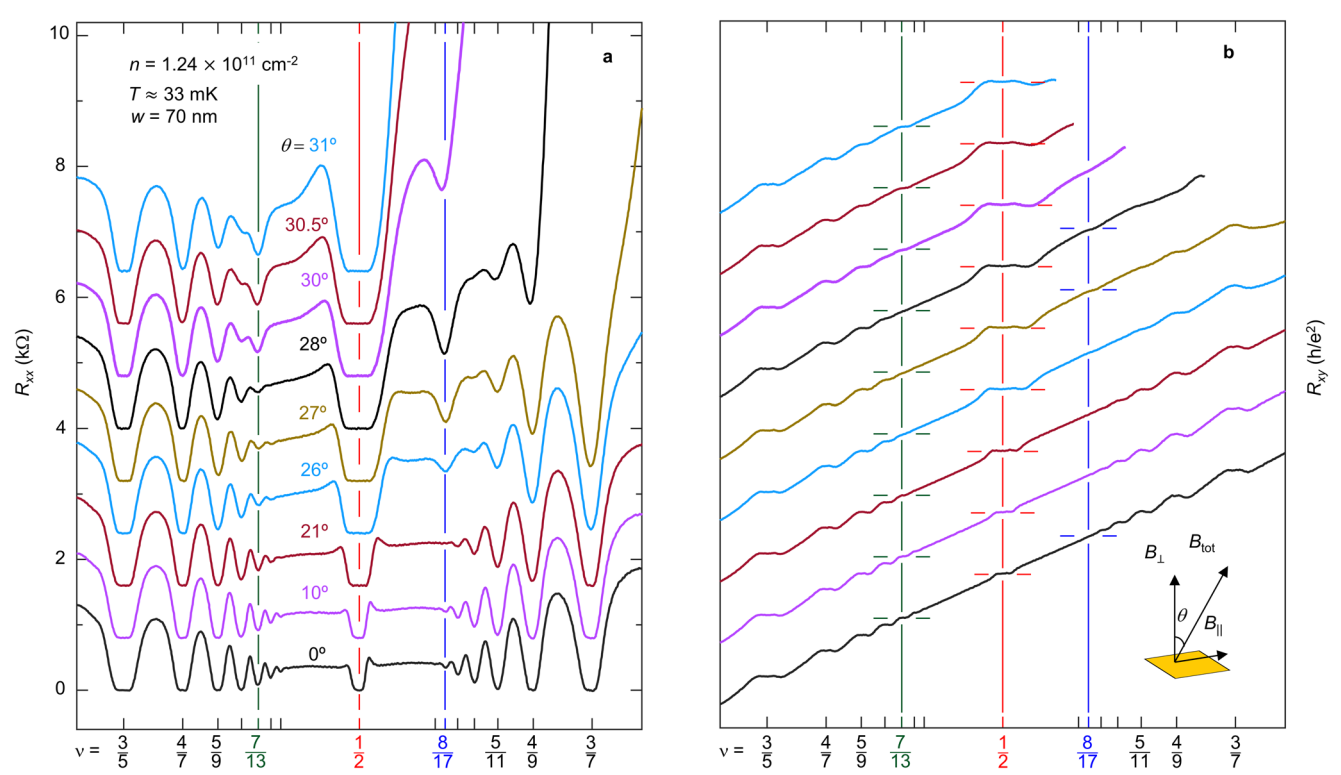
The inset shows the self-consistently calculated charge distribution for  $2.80\,(black)$  and  $3.26\times10^{11}\,cm^{-2}\,(green)$ . **b**, Experimentally determined phase diagram depicting the phase boundaries between the composite fermion Fermi sea and the  $1/2\,FQHS$ , and the  $1/2\,FQHS$  and insulating phase, by dashed and dotted lines, respectively. The  $1/2\,FQHS$  is stable for an intermediate density range, and is sandwiched between the compressible composite fermion Fermi sea at low densities and the incompressible insulating phase at high densities. Within the intermediate density range, as the density is increased away from the compressible boundary, the  $1/2\,FQHS$  gets stronger, but eventually begins to weaken as the nearby insulating phase begins to engulfit; see Ref. 22 for details. Figure reproduced with permission from ref. 22, APS.



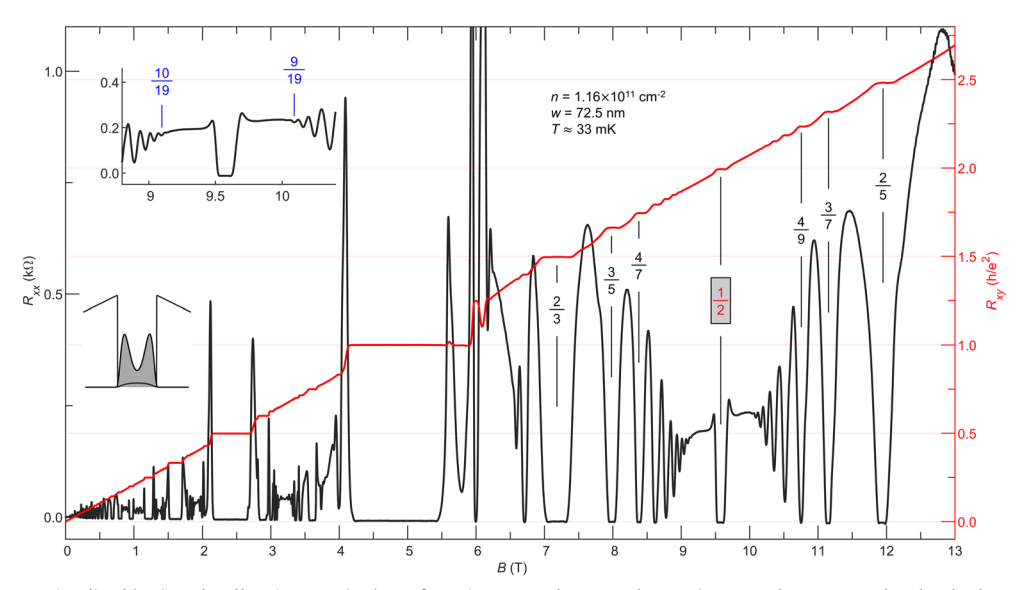
**Extended Data Fig. 2** | **Evolution of an electron system in a 70-nm-wide GaAs QW with varying density. a,b**, Longitudinal  $(R_{xx})$  and Hall resistance  $(R_{xy})$  as a function of 1/v in a 70-nm-wide GaAs QW. Traces are offset vertically for clarity.  $R_{xx}$  for the lowest density n=1.09 shows a compressible v=1/2 composite fermion Fermi sea, with the characteristic Jain-sequence states up to v=10/19 and 9/19 on its flanks. Note that the  $R_{xx}$  minima at v=8/17 and 7/13 are strong, but their strength relative to other, nearby FQHSs is consistent with what is expected for Jain-sequence states. As the density is increased, the compressible composite fermion Fermi sea makes a transition into an incompressible FQHS at v=1/2, which gets stronger as the density is further



raised. The odd-denominator FQHSs flanking the 1/2 FQHS undergo a similar evolution as displayed in Fig. 1e, where the Jain-sequence states get weaker because of the increased electron layer thickness, but the 8/17 and 7/13 FQHSs suddenly transition into anomalously strong FQHSs, distinct from Jain-sequence states. Quantitatively, owing to the smaller well width, the transitions of the  $\nu=8/17$  and 7/13 FQHSs are both shifted to higher densities compared to the 72.5-nm-wide sample of Fig. 1. In panel **b**, self-consistently calculated charge distributions for a 2DES confined to a 70-nm-wide GaAs QW at n=1.24 and  $1.60 \times 10^{11}$  cm<sup>-2</sup> are shown as bottom and top insets, respectively.

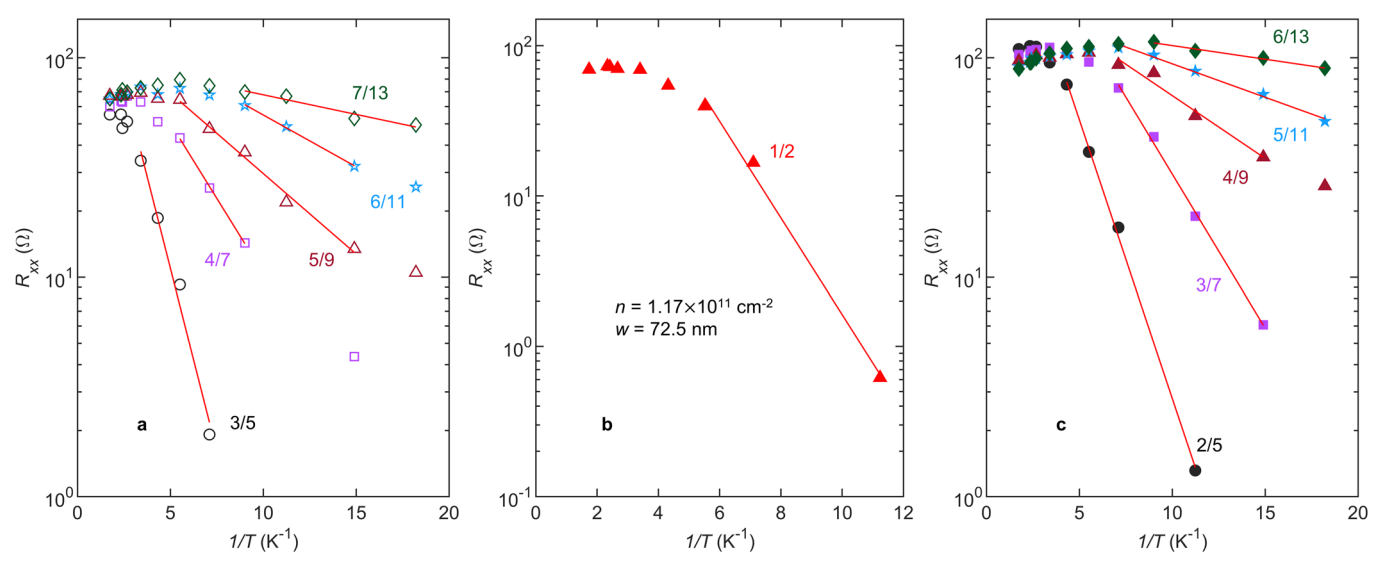


**Extended Data Fig. 3** | **Evolution of an electron system in a 70-nm-wide GaAs QW with in-plane magnetic field. a,b**, Longitudinal ( $R_{xx}$ ) and Hall ( $R_{xy}$ ) resistances are shown as a function of 1/ $\nu$  at various tilt angles for  $n = 1.24 \times 10^{11}$  cm<sup>-2</sup>. Qualitatively, once again the sample shows a similar evolution of FQHSs at and around  $\nu = 1/2$  as the 72.5-nm-wide sample, albeit at higher tilt angles.



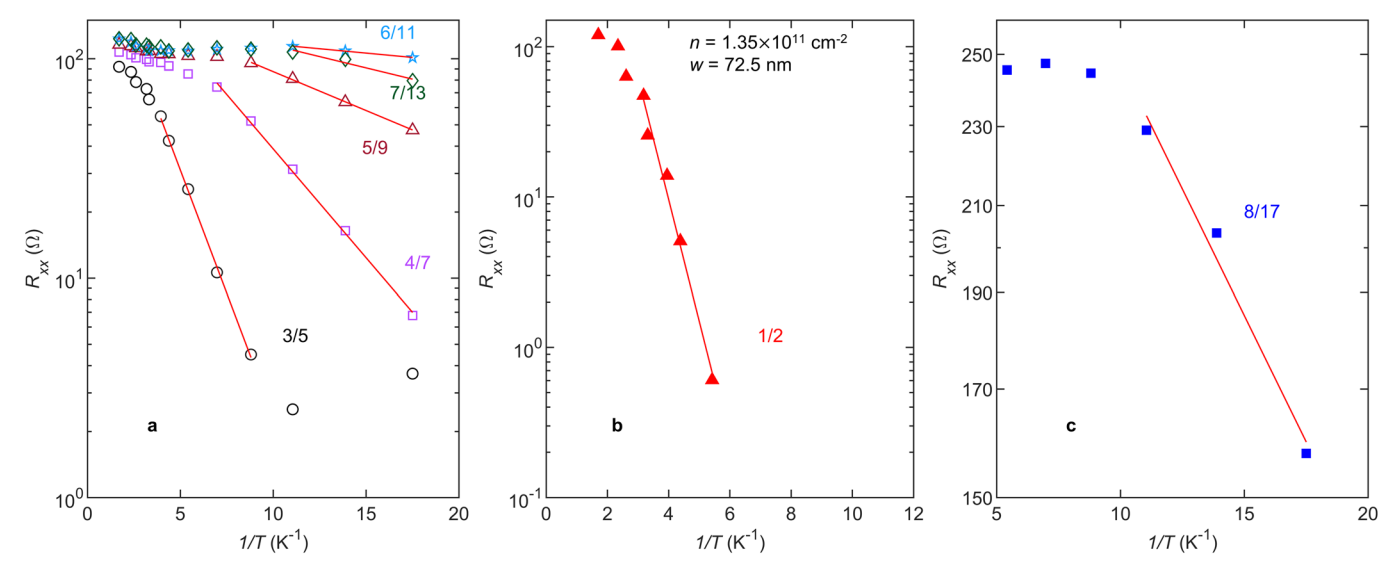
Extended Data Fig. 4 | Longitudinal ( $R_{xy}$ ) and Hall resistance ( $R_{xy}$ ) as a function of perpendicular magnetic field for ultrahigh quality 2D electrons in a 72.5-nm-wide GaAs QW. The strong FQHS observed at  $\nu=1/2$  and flanked by numerous high-order Jain-sequence FQHSs up to  $\nu=9/19$  and 10/19 (as shown

in the top right inset) on its sides attest to the ultra high quality of our sample. Top left inset shows the self-consistently calculated charge distribution for  $n=1.16\times 10^{11}\,\mathrm{cm^{-2}}$  electrons confined to a 72.5-nm-wide GaAs QW.



Extended Data Fig. 5 | Arrhenius plots to extract the energy gaps of FQHSs in the N=0 LL for n=1.17. a-c, Temperature dependence of  $R_{xx}$  minima for the FQHSs on the low-field side of v=1/2, at v=1/2, and on the high-field side of v=1/2, respectively. The red lines through the data points are fits to the data points in the activated regimes for different fillings, and their slopes yield the energy gaps  $\Delta_{v}$ , determined from  $R_{xx} \propto e^{-\Delta_{v}/2kT}$ . Note in panel a that the v=7/13

FQHS is weaker than the 6/11 FQHS and has a smaller energy gap. The activated behavior of  $R_{\rm xx}$  at the different FQHSs allows us to extract an energy gap, but one must be careful with the energy gaps of the weakest FQHSs which mostly serve as a measure of their strength. Because of the limited available temperature range and the effect of disorder, the small energy gaps of the higher-order FQHSs have a large error bar.



Extended Data Fig. 6 | Arrhenius plots to extract the energy gaps of FQHSs in the N=0 LL for n=1.35. Data are for the 72.5-nm-wide GaAs QW with  $n=1.35\times 10^{11}$  cm $^{-2}$ . a-c, Temperature dependence of  $R_{xx}$  minima for the FQHSs on the low-field side of v=1/2, at v=1/2, and on the high-field side of v=1/2, respectively. The red lines through the data points are fits to the data points in

the activated regimes for different fillings, and their slopes yield the energy gaps  $\Delta_{\nu}$ , determined from  $R_{xx} \propto e^{-\Delta v/2kT}$ . Note in panel **a** that, at this density, the 7/13 FQHS has a larger gap than the 6/11 FQHS. On the high-field side of v=1/2 (panel **c**), only the v=8/17 FQHS yields an activation, and the other FQHSs at higher fields are consumed by the ensuing insulating phase; see Fig. 1e of main text.